Modulation of the muscarinic K^+ channel by P_2-purinoceptors in guinea-pig atrial myocytes

Hiroshi Matsuura and Tsuguhisa Ehara

Department of Physiology, Saga Medical School, Saga 849, Japan

1. Activation of muscarinic K^+ (K_{ACh}) channels by P_2-purinergic agonists, such as ATP, decreases monotonically in the continued presence of agonist. We investigated the mechanisms underlying this process of decline in guinea-pig atrial myocytes using the patch-clamp technique.

2. External ATP reversibly depressed the acetylcholine (ACh, 5·5–11 μM)-induced K_{ACh} current in a concentration-dependent manner with a half-maximal inhibitory concentration (IC_{50}) of 5·4 μM.

3. External ATP irreversibly reduced guanosine-5′-*O*-(3-thiotriphosphate) (GTPγS)-induced K_{ACh} current both in control and pertussis toxin (PTX)-pretreated cells, suggesting (i) that the ATP-induced inhibition of K_{ACh} current occurred at some step(s) downstream from the activation of the PTX-sensitive G protein, G_K, and (ii) that a PTX-insensitive G protein was involved in the signal transduction pathway.

4. The potency order of ATP analogues in reducing K_{ACh} current was ATP $\geqslant$ 2-methylthio-ATP $\geqslant$ α,β-methylene-ATP, indicating involvement of a P_{2Y}-type purinoceptor.

5. In the cell-attached patch recording, ATP (100 μM) applied to the bath solution reduced the activity of the K_{ACh} channels activated by ACh in the pipette, in two out of eight experiments, suggesting the possible involvement of cytosolic second messengers in the inhibition of K_{ACh} channels.

6. The ATP-induced reduction of K_{ACh} current was not affected by a protein kinase C inhibitor, 1-(5-isoquinolinesulphonyl)-2-methylpiperazine dihydrochloride (H-7), suggesting that this response was not mediated by the activation of protein kinase C.

7. These results demonstrate that, in addition to the membrane-delimited activation through G_K, external ATP causes an inhibition of the K_{ACh} channel probably by activating a PTX-insensitive G protein and cytosolic second messenger(s), which may underlie the monotonic decrease of the ATP-activated K_{ACh} current.

In the heart, activation of the muscarinic K^+ (K_{ACh}) channel by acetylcholine (ACh) via muscarinic (M_2) receptors is primarily associated with a negative chronotropism caused by vagal activity. The K_{ACh} channel was shown to be regulated by a pertussis toxin (PTX)-sensitive G protein, G_K, in a membrane-delimited manner in cardiac atrial cell membrane (Pfaffinger, Martin, Hunter, Nathanson & Hille, 1985; Breitwieser & Szabo, 1985; Kurachi, Nakajima & Sugimoto, 1986). The occupancy of the muscarinic receptor by ACh causes the G protein, G_K, to release GDP, bind GTP, and dissociate into an α-GTP subunit and a $\beta\gamma$ subunit which is responsible for the physiological activation of the K_{ACh} channel (Logothetis, Kurachi, Galper, Neer & Clapham, 1987; for review, see Kurachi, 1995). In addition to the muscarinic receptor, receptors for P_1-purinergic agonists (Kurachi *et al.* 1986), somatostatin (Lewis & Claphan, 1989), calcitonin gene-related peptide (Kim, 1991*a*) and endothelin (Kim, 1991*b*) have also been shown to interact directly with the G_K–K_{ACh} channel system in atrial cell membrane. One characteristic feature of the K_{ACh} current is its 'desensitizing' property. Previous studies have demonstrated that K_{ACh} current activated via muscarinic or P_1-purinergic receptors diminishes in the continued presence of agonists, which was demonstrated to involve agonist-induced functional alterations of the receptors (Carmeliet & Mubagwa, 1986; Kwatra & Hosey, 1986), G protein (G_K; Kurachi, Nakajima & Sugimoto, 1987) or the K^+ channel proteins (Kim, 1991*c*).

The P_2-purinoceptor has recently been suggested to be coupled to the K_{ACh} channel through G_K in guinea-pig atrial cell membranes (Matsuura, Sakaguchi, Tsuruhara & Ehara, 1996), analogous to the coupling mechanism of the muscarinic receptor to this channel. However, the activity of the K_{ACh} channels induced by P_2-purinergic agonists, such as ATP, rapidly subsides in the continued presence of the agonist; the response completely disappears during a 2 min

exposure to ATP at a concentration of 1 μM, which is lower than the half-maximal concentration of ATP (1·84 μM) required for activation. Such a complete decline was not observed in the responses evoked by ACh or adenosine, even at very high concentrations, such as 110 μM ACh (Kurachi *et al.* 1987). This clear difference led us to examine the possibility that ATP may evoke an inhibitory action on the K_{ACh} channel, although we simply interpreted this ATP-induced process of decline in the previous report (Matsuura *et al.* 1996) as a desensitization-like phenomenon. The present study demonstrates that P_2-purinoceptor stimulation not only activates the K_{ACh} channel via a membrane-delimited mechanism involving G_K, but also initiates a second inhibitory action on this channel, which is probably mediated by a distinct PTX-insensitive G protein and cytosolic second messenger(s).

METHODS

Cell preparation

Atrial cells were obtained from guinea-pig hearts using an enzymatic dissociation procedure similar to that described by Powell, Terrar & Twist (1980). Briefly, guinea-pigs (250–400 g body weight) were killed by a sodium pentobarbitone overdose (120 mg kg^{-1} I.P.) and thereafter a thoracotomy was performed. Hearts were Langendorff perfused, initially with normal Tyrode solution containing 3 U l^{-1} heparin, then for 5 min with nominally Ca^{2+}-free Tyrode solution (approximately 1–2 μM free [Ca^{2+}]), and finally for 5–10 min with nominally Ca^{2+}-free Tyrode solution containing 0·5 mg ml^{-1} collagenase (Wako Pure Chemical Industries, Osaka, Japan). Hearts were then removed from the perfusion apparatus and the digested atrium was mechanically agitated to disperse the myocytes. Isolated myocytes thus obtained were stored at 4 °C in a high-K^+, low-Cl^- Kraftbrühe (KB) solution (Isenberg & Klöckner, 1982) until use. Spindle-like quiescent atrial cells with clear striations were used in the experiments.

Voltage-clamp technique

Single atrial cells were voltage clamped using 'whole-cell' and 'cell-attached' configurations of the patch-clamp technique (Hamill, Marty, Neher, Sakmann & Sigworth, 1981) with an EPC-7 patch-clamp amplifier (List). Patch electrodes were made from glass capillaries (o.d. 1·5 mm, i.d. 1·0 mm; Narishige) using a horizontal microelectrode puller (P-80/PC; Sutter Instrument Co., Novato, CA, USA), and the tips were fire polished with a microforge. Electrode tip resistance ranged from 2·0 to 2·5 MΩ for the whole-cell recording and from 5·0 to 8·0 MΩ for the cell-attached single-channel recording, when filled with the respective pipette solutions. Isolated atrial myocytes were allowed to settle onto the glass bottom of a recording chamber (0·5 ml in volume) mounted on the stage of an inverted microscope (Nikon Diaphot). The chamber was maintained at 34–36 °C and was continuously perfused at a rate of 2–3 ml min^{-1} with Tyrode solution. Current and voltage signals were stored on digital audiotape (DT-120; Sony) using a PCM data recorder (RD-101T; TEAC, Tokyo, Japan) for subsequent computer analysis (PC98RL; NEC, Tokyo, Japan). Current records were fed to the computer every 0·5 ms for the analysis of whole-cell currents and every 0·2 ms for analysis of single-channel currents, through a low-pass filter (48 dB per octave, E-3201A; NF Electronic Instruments, Yokohama, Japan) at an appropriate cut-off frequency. Cell membrane capacitance was measured by the integral of the charging transient in response to a 5 or 10 mV step pulse in voltage-clamp conditions. Data are given as means ± S.E.M. Statistical comparisons were made using Student's t test, and differences were considered to be significant at $P < 0·05$.

Solutions

Normal Tyrode solution contained (mM): NaCl, 140; NaH_2PO_4, 0·33; KCl, 5·4; $CaCl_2$, 1·8; $MgCl_2$, 0·5; glucose, 5·5; Hepes, 5·0 (pH adjusted to 7·4 with NaOH). The nominally Ca^{2+}-free Tyrode solution used for the cell isolation procedure was prepared by simply omitting $CaCl_2$ from the normal Tyrode solution. The external solution for the measurement of whole-cell K_{ACh} current was normal Tyrode solution plus 0·1 mM $CdCl_2$. Agents added to the external solutions included ATP (disodium salt; Sigma), ACh (sodium salt; Daiichi Seiyaku, Tokyo, Japan), adenosine (sodium salt; Sigma), 2-methylthio-ATP (tetrasodium salt; Research Biochemicals Inc.), and α,β-methylene-ATP (lithium salt; Sigma). The control pipette solution used for the whole-cell recording contained (mM): potassium aspartate, 70; KCl, 50; KH_2PO_4, 10; $MgSO_4$, 1; Na_2-ATP, 3; Li_2-GTP, 0·1; EGTA, 5; Hepes, 5 (pH adjusted to 7·2 with KOH). The amount of KOH required for titration, measured in several experiments, was found to average 24 mM. Therefore, the total K^+ concentration in the control pipette solution was 154 mM. In some experiments, 5 mM EGTA in the pipette solution was replaced by 20 mM 1,2-bis(2-aminophenoxy)-ethane-*N,N,N′,N′*-tetraacetic acid (BAPTA; Dojindo Laboratories, Kumamoto, Japan). The concentrations of intracellular free Ca^{2+} with 5 mM EGTA and 20 mM BAPTA were estimated to be approximately $6·0 \times 10^{-11}$ M (pCa = 10·2) and $2·0 \times 10^{-11}$ M (pCa = 10·7), respectively (Fabiato & Fabiato, 1979; Tsien, 1980; Tsien & Rink, 1980). GTP at a concentration of 100 μM in the pipette solution was replaced by 100 or 200 μM guanosine-5′-*O*-(3-thiotriphosphate) (GTPγS, tetralithium salt; Boehringer Mannheim) in some experiments. The pipette solution used for the cell-attached single-channel recording contained (mM): KCl, 140; $CaCl_2$, 1·8; Hepes, 5·0 (pH adjusted to 7·4 with KOH). The KB solution for cell preservation contained (mM): potassium glutamate, 70; KCl, 30; KH_2PO_4, 10; $MgCl_2$, 1; taurine, 20; EGTA, 0·3; glucose, 10; Hepes, 10 (pH adjusted to 7·2 with KOH). Pertussis toxin (200 μg ml^{-1}; Seikagaku Corporation, Tokyo, Japan) was dissolved in KB solution for cell incubation at a final concentration of 5 μg ml^{-1} (Hwang, Horie, Nairn & Gadsby, 1992). To inhibit protein kinase C, 1-(5-isoquinolinesulphonyl)-2-methylpiperazine dihydrochloride (H-7; Seikagaku Corporation) was added to the pipette solution.

RESULTS

Comparison of ATP- and ACh-induced K_{ACh} current

Activation of K_{ACh} current by stimulation of P_2-purinoceptors was characterized by a monotonic decrease despite the continuous presence of the agonists (Matsuura *et al.* 1996). In the experiment shown in Fig. 1, we compared the changes in the amplitude of K_{ACh} current activated by ATP with that activated by ACh in the presence of each agonist. External application of 50 μM ATP caused an outward shift of the holding current at −40 mV, which then rapidly declined to a steady level (Fig. 1*A*). It should be noted that this final steady level was below the pre-drug level (a late inward shift of the holding current). After washing out the ATP, this inward shift of the holding current gradually returned to the control level. The cell was then exposed to 10 μM ACh with a 7 min washout period. In order to clarify

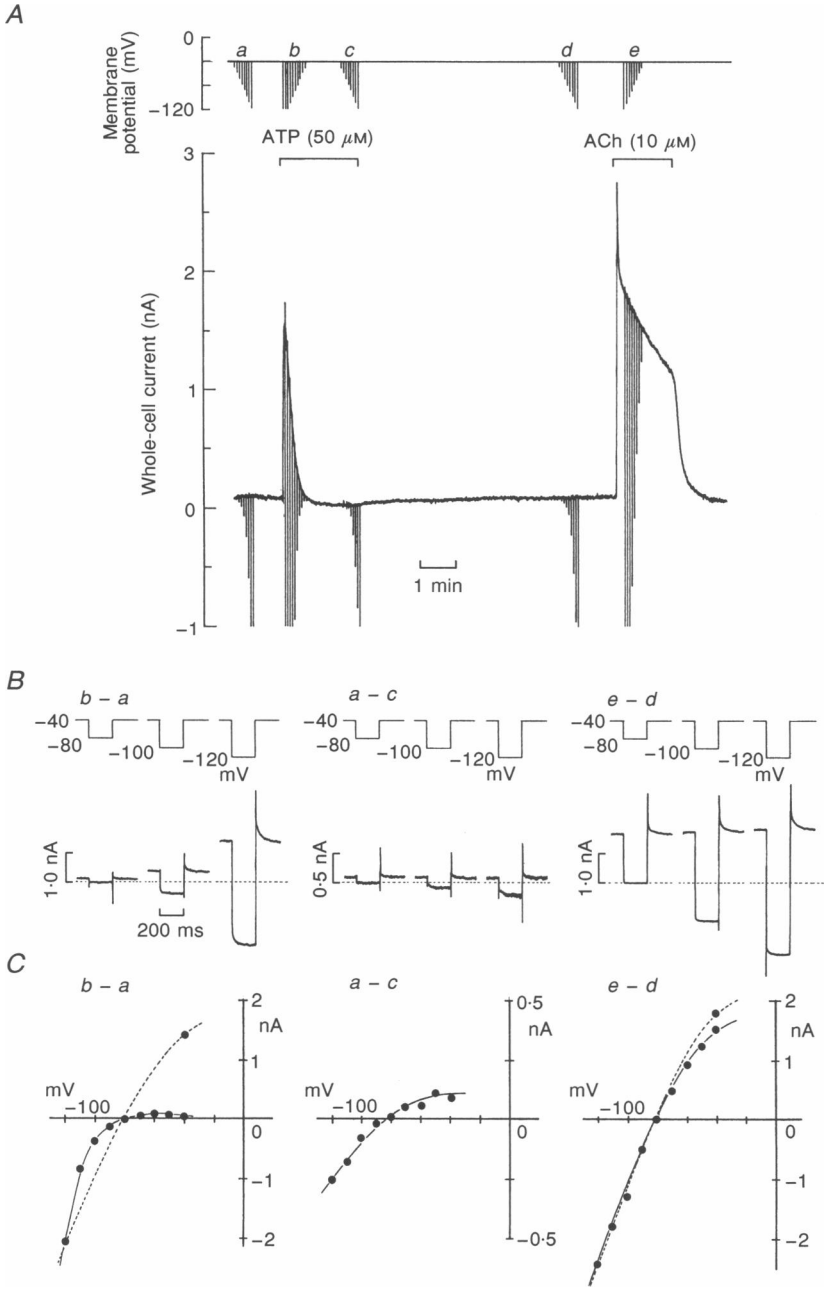

Figure 1. Effects of ATP and ACh on whole-cell membrane currents

A, chart records of membrane potential (upper trace) and whole-cell current (lower trace). The cell was successively exposed to 50 μM ATP and 10 μM ACh, as indicated by the horizontal bars over the chart record. Theophylline (500 μM) was present during the application of ATP to block P_1-purinoceptors. Vertical lines in upper trace show application of 200 ms voltage pulses to potentials between −50 and −120 mV in 10 mV steps from a holding potential of −40 mV, and deflections in lower trace represent the resulting current changes. Note differences in the holding current levels upon the imposition of each test pulse observed both in ATP and ACh exposure. *B*, expanded current traces of ATP-induced ($b - a$), ATP-inhibited ($a - c$) and ACh-induced currents ($e - d$) in response to voltage steps to −80, −100 and −120 mV, obtained by subtraction of corresponding digitized records in *A*. *C*, current–voltage (I–V) relationships of ATP-induced ($b - a$), ATP-inhibited ($a - c$) and ACh-induced currents ($e - d$), measured near the end of each pulse, obtained from *B*. For the ATP-induced ($b - a$) and ACh-induced currents ($e - d$), both the maximal and minimal current amplitudes are plotted at the −40 mV holding potential. Continuous and dashed lines through data points were fitted by eye using the minimal and maximal values at the −40 mV holding potential, respectively. Cell capacitance was 69·09 pF.

the nature of the membrane currents responsible for the initial outward and the late inward shifts of the holding current in the presence of ATP, the difference currents during hyperpolarizing test potentials were obtained by digital subtraction. The ATP-induced current associated with the initial outward shift of the holding current, obtained by subtracting the currents recorded under control conditions from those during exposure to ATP ($b - a$), exhibited relaxations during stepwise changes of whole-cell membrane potentials (Fig. 1*B*, left panel), an inward-going rectification and a reversal potential of −80 mV, close to the potassium equilibrium potential ($E_K = -88{\cdot}2$ mV, Fig. 1*C*, left panel), confirming the ATP-induced activation of K_{ACh} current. Since the ATP-induced outward current decreased rapidly, the holding current level of the difference current was not constant during the time at which test pulses were applied (Fig. 1*B*, left panel).

The membrane current components responsible for the late inward shift of the holding current in the presence of ATP, obtained by subtracting the membrane currents recorded in the later stage of ATP application from those of control ($a - c$), were also characterized by relaxations on voltage jumps (Fig. 1*B*, middle panel), an inward rectification and high K^+ selectivity as judged by the reversal potential (−80 mV) near E_K (Fig. 1*C*, middle panel), showing an involvement of K_{ACh} current. This finding strongly suggests the following two points. Firstly, there was an outward current through the K_{ACh} channel at −40 mV holding potential even in agonist-free conditions (basal activity of the K_{ACh} channel; Sakmann, Noma & Trautwein, 1983). Secondly, a suppression of this basal activity occurred in the continuous presence of ATP, which led to the net inward shift of the holding current at −40 mV. Thus, K_{ACh} current was found to be initially activated and then depressed

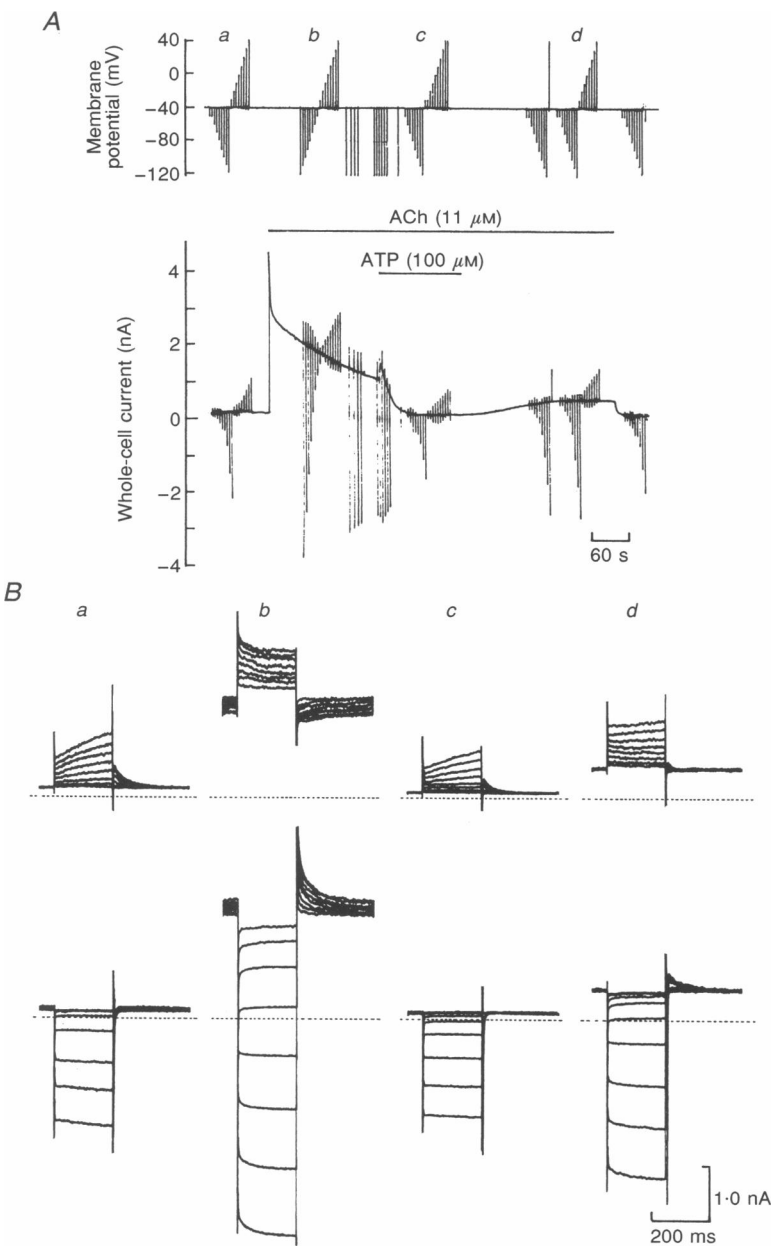

Figure 2. Effects of ATP on ACh-induced K_{ACh} current

A, chart records of membrane potential (upper trace) and whole-cell current (lower trace). Bars above the current record mark periods of external application of 11 μM ACh and 100 μM ATP. Vertical lines in upper trace show application of 200 ms voltage pulses to potentials between +40 and −120 mV in 10 mV steps from a holding potential of −40 mV, and deflections in lower trace represent the resulting current changes. Note that the holding current level in the presence of ACh + ATP was more negative than the control level. *B*, expanded current traces in response to 200 ms of depolarizing (upper traces) and hyperpolarizing test pulses (lower traces) in *A*, before (*a*) and during (*b*) exposure to ACh, after addition of ATP (*c*), and after withdrawal of the ATP in the presence of ACh (*d*). Zero-current level is indicated by dotted lines in each panel. Cell capacitance was 88·32 pF.

during exposure to ATP. The times required to reach a peak activation and a peak depression of K_{ACh} current after application of 50 μM ATP were 2·5 ± 0·2 s and 76·4 ± 4·7 s ($n = 5$), respectively.

As expected, exposure to 10 μM ACh activated K_{ACh} current, identified by its voltage-jump relaxations (Fig. 1*B*, right panel), reversal potential near E_K and inward rectification (Fig. 1*C*, right panel), which exhibited two phases of desensitization, i.e. the rapid phase appearing within the first 20 s and the secondary slower phase continuing over a few minutes (Kurachi *et al.* 1987; Kim, 1991*c*). ACh and adenosine never produced a net inward shift of the holding current even after 5 min exposure (data not shown), in agreement with observations of other investigators (Zang, Yu, Honjo, Kirby & Boyett, 1993). We then examined whether extracellular ATP can depress K_{ACh} current activated by other agonists, such as ACh and adenosine.

Inhibition of ACh-induced K_{ACh} current by ATP

Figure 2 shows the results of an experiment in which the interactions of ATP and ACh on the membrane currents were examined. In this experiment, the typical K_{ACh} current response was initially evoked by a bath application of 11 μM ACh, and then 100 μM ATP was added to the bathing solution about 3 min after starting the ACh application. It was found that, although ATP initially increased the outward holding current to a slight extent, it then rapidly depressed the ACh response. The depression was so marked that the holding current level became more negative than the control, i.e. the level before ACh application. When ATP was withdrawn, the holding current gradually shifted outwardly, suggesting that the effects of ATP on the membrane currents were at least partly reversible. The initial outward shift of the holding current on application of ATP is probably due to an additional activation of K_{ACh} current. This point will be

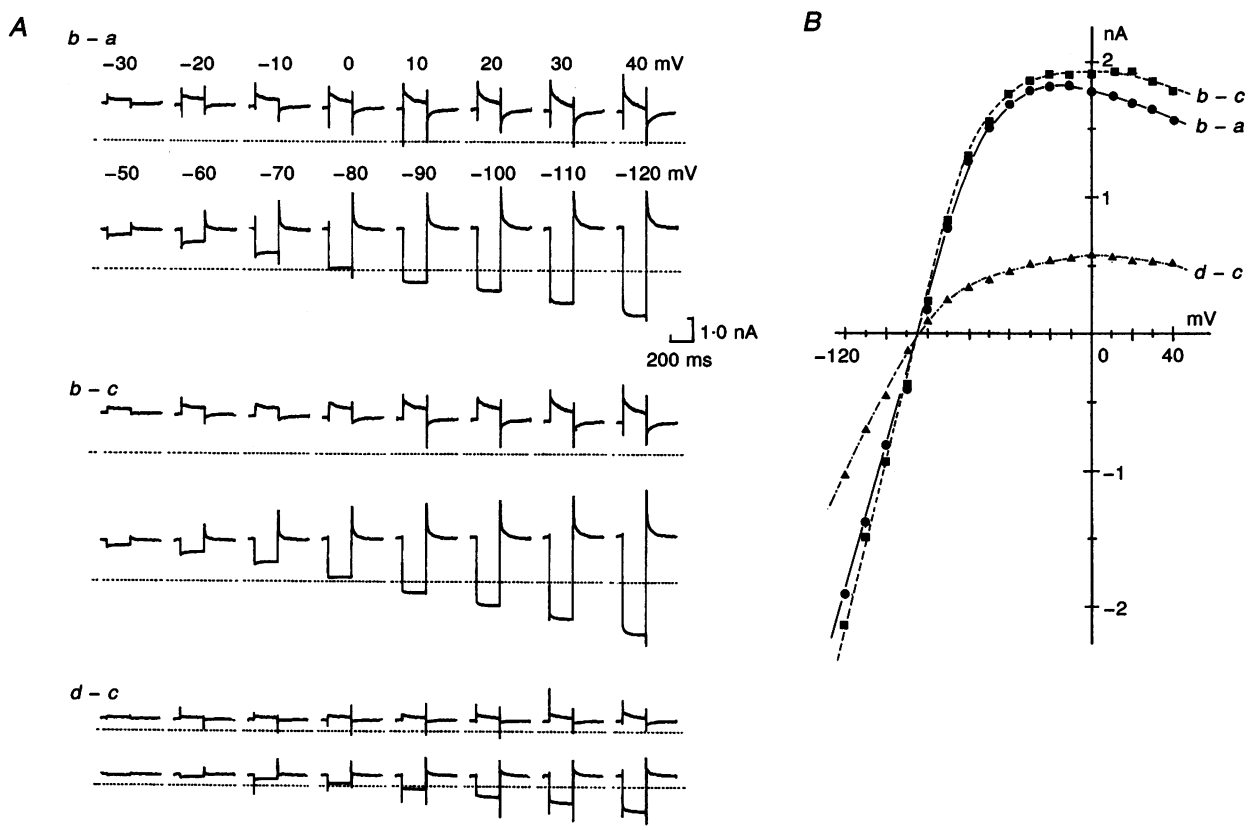

Figure 3. Inhibition of K_{ACh} current by ATP from the experiment of Fig. 2

A: top panel shows ACh-induced current ($b - a$), obtained by digital subtraction, at each test potential shown above the current trace; middle panel illustrates the membrane currents inhibited by ATP ($b - c$), determined by digital subtraction of the current trace recorded in the presence of ACh + ATP (c) from that in the presence of ACh (b) at each test potential; bottom panel demonstrates membrane current which recovered after withdrawal of the ATP ($d - c$), determined by digital subtraction of the current trace in the presence of ACh + ATP (c) from that recorded in the presence of ACh after withdrawal of ATP (d), at each test potential. Zero-current level is indicated by dotted lines in each trace. *B*, *I–V* relationships of ACh-induced current ($b - a$, ●), ATP-inhibited current ($b - c$, ■), and membrane current which recovered after withdrawal of ATP in the presence of ACh ($d - c$, ▲).

discussed further later (Fig. 5). Figure 2*B* illustrates the membrane currents in response to depolarizing (upper traces) and hyperpolarizing test potentials (lower traces) recorded before (*a*) and during (*b*) exposure to ACh, after addition of ATP (*c*), and after withdrawal of ATP in the presence of ACh (*d*).

To clarify the nature of the membrane currents affected by ACh and ATP, agonist-induced difference currents were obtained by computer subtraction (Fig. 3*A*). The ACh-induced currents (Fig. 3*A*; *b* − *a*) exhibited relaxations upon voltage jumps, a reversal potential of −84 mV and an inward rectification (Fig. 3*B*; *b* − *a*, ●) confirming the ACh-induced activation of K_{ACh} current. The membrane current components depressed by ATP in the presence of ACh (Fig. 3*A* and *B*; *b* − *c*, ■) also showed characteristics similar to those of ACh-induced K_{ACh} current, indicating that external ATP depressed ACh-induced K_{ACh} current. In addition, the amplitude of K_{ACh} current inhibited by ATP was greater than that activated by ACh alone over the entire voltage range examined (Fig. 3*B*), indicating that ATP totally inhibits ACh-induced K_{ACh} current as well as its basal activity. The degree of inhibition, obtained by normalizing the magnitude of the membrane current inhibited by ATP (Fig. 3*B*; *b* − *c*, ■) with reference to the amplitude of K_{ACh} current activated by ACh (Fig. 3*B*; *b* − *a*, ●) at each test potential, ranged from 104 to 112%, showing no significant voltage dependence of ATP-induced depression. A similar inhibition by ATP (100 μM) of K_{ACh} current induced by ACh (11 μM) over the entire voltage range (+40 to −120 mV) was consistently observed in a total of five myocytes, the mean inhibition being 96·3 ± 8·1% at −40 mV (cf. Fig. 8). The time required to reach a peak depression after application of 100 μM ATP was 63·0 ± 2·6 s ($n = 5$, Fig. 2*A*). The membrane current that recovered after withdrawal of ATP (Fig. 3*A* and *B*; *d* − *c*, ▲) can also be identified as K_{ACh} current by its electrophysiological properties (voltage-jump relaxations, reversal potential near E_K and inward rectification), showing again that ATP-induced depression was, at least in part, reversible. A similar depression by ATP was also observed in K_{ACh} current induced by adenosine (100 μM) ($n = 3$, data not shown), indicating that the ATP-induced depression of K_{ACh} current was not specific for the muscarinic receptor-mediated activation.

Inhibition of GTPγS-induced K_{ACh} current by ATP

We then examined the effects of ATP on K_{ACh} current induced by direct activation of G_K with the intracellular application of non-hydrolysable GTP analogue. In the experiment shown in Fig. 4, the pipette solution contained 200 μM GTPγS in place of GTP. Soon after the membrane patch was ruptured, the outward holding current started to increase at the −50 mV holding potential associated with the activation of the K_{ACh} channel (Fig. 4*A*), as expected (Kurachi *et al.* 1987). When the outward current response reached a steady state, 10 μM ATP was added to the bath solution. ATP initially increased and then depressed the outward holding current, the depression persisting after withdrawal of ATP (cf. Fig. 2*A*). After a 3·5 min washout period, 10 μM ACh was applied to the cell, which did not affect the holding current (Fig. 4*A* and *B*), as expected from the hypothesis that the muscarinic receptor is functionally uncoupled from its associated G protein (G_K) by non-hydrolysable GTP analogues (Breitwieser & Szabo, 1985; Kurachi *et al.* 1987). Figure 4*B* illustrates the membrane currents in response to depolarizing (upper traces) and hyperpolarizing test potentials (lower traces) recorded at the times indicated by *a*–*f* on the chart record (Fig. 4*A*).

The membrane current components inhibited by ATP, obtained by subtraction, exhibited relaxation on voltage jumps (Fig. 5*B*; *a* − *c*), a reversal potential of −84 mV and an inward rectification (Fig. 5*D*; *a* − *c*, ●), indicating that GTPγS-induced K_{ACh} current was also inhibited by ATP over the full voltage range. The degree of inhibition, obtained by normalizing the magnitude of the inward current shift at −50 mV caused by ATP (0·633 nA) with reference to the amplitude of the outward current activated by intracellular GTPγS (0·846 nA), was 75% in this example. The time required to reach peak inhibition after application of ATP was 72 s (Fig. 4*A*). The result that ATP inhibited K_{ACh} current induced by direct activation of G_K with intracellular GTPγS indicates that ATP-induced inhibition occurred at some step(s) downstream from the activation of G_K.

The persistent inhibition of K_{ACh} current by ATP was consistently observed in all myocytes loaded with GTPγS ($n = 21$), which was in marked contrast to the reversible inhibition observed in cells loaded with GTP (Figs 2 and 3). If the ATP-induced response is dependent upon turnover of a certain G protein, hydrolysis of GTP on Gα to GDP by GTPase and subsequent reassociation of $G\alpha_{GDP}$ with $G\beta\gamma$ into the heterotrimeric form should lead to cessation of the response (Gilman, 1987). Since GTPγS cannot be hydrolysed by the GTPase of Gα, the G protein-mediated response is expected to persist in cells loaded with GTPγS due to perpetual dissociation of subunits (Jakobs, Gehring, Gaugler, Pfeuffer & Schultz, 1983; Gilman, 1987), as clearly demonstrated for cardiac β-adrenoceptor-mediated Cl^- current activation involving G_S (Hwang *et al.* 1992). It seems reasonable, therefore, to interpret the persistent inhibition by ATP in the GTPγS-loaded myocyte (Figs 4 and 5) as representing an involvement of a class of G protein in the signal transduction system mediating the ATP-induced inhibition of K_{ACh} current.

As mentioned before (Fig. 2), the initial transient increase in the outward current observed upon ATP application could be due to an additional activation of K_{ACh} current. However, the difference current obtained at this phase (Fig. 5*A*; *b* − *a*) was different from that expected for K_{ACh} current: the inward current in response to a hyperpolarizing pulse showed a rapid decay, although the outward current on return to the −50 mV holding potential showed a relaxation-like decline. It is, therefore, possible that another

current component was involved in the response. In relation to this, ATP is also known to activate a current through non-selective cation channels which declines rapidly after activation (rapid desensitization) in guinea-pig atrial cells (Hirano, Abe, Sawanobori & Hiraoka, 1991; Matsuura & Ehara, 1992). At a negative membrane potential, this current should appear as a rapidly decaying inward current. Thus, we assume that during a short period after application of ATP there was a concurrent activation of this current component and K_{ACh} current, which resulted in the complicated feature of the current trace observed (Fig. 5*A*).

We previously showed that the P_2-purinoceptor is coupled to the K_{ACh} channel via a PTX-sensitive G protein (G_K) to activate K_{ACh} current (cf. Fig. 1) in guinea-pig atrial myocytes (Matsuura *et al.* 1996). To characterize the G protein involved in the ATP-induced inhibition of K_{ACh} current, we tested whether ATP can inhibit K_{ACh} current in PTX-pretreated cells. Cells were pre-incubated at 32 °C for 2 h in a KB solution containing 5 μg ml^{-1} PTX. Inhibition of PTX-sensitive G proteins after this PTX treatment was confirmed by the inability of ACh (5·5 μM) to activate K_{ACh} current in these atrial myocytes (data not shown). In the

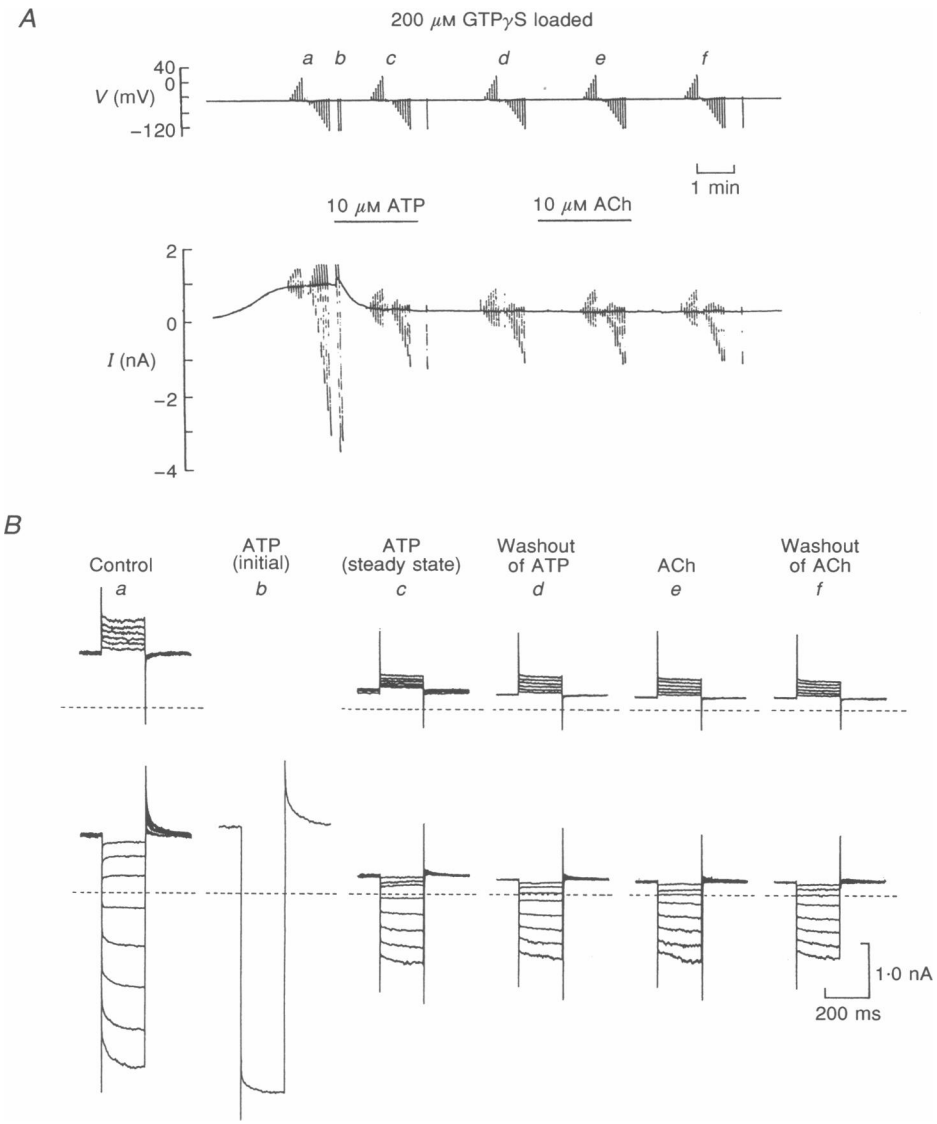

Figure 4. Effects of external ATP on GTPγS-induced K_{ACh} current

The cell was loaded intracellularly with 200 μM GTPγS through a pipette. *A*, chart record of membrane potential (upper trace) and whole-cell current (lower trace). The chart recording of whole-cell current was begun just after the membrane patch was ruptured to start intracellular dialysis with 200 μM GTPγS. Periods of exposure to 10 μM ATP and 10 μM ACh are indicated by the horizontal bars over the current record. *B*, superimposed current traces in response to 200 ms voltage steps to membrane potentials of −40 to +10 mV (upper traces), and −60 to −130 mV (lower traces) in 10 mV steps applied from a holding potential of −50 mV at the times indicated by the corresponding letters (*a*, *c*, *d*, *e* and *f*) above the voltage record in *A*. The membrane current in response to a voltage step to −130 mV recorded at the point marked *b* is also shown. Cell capacitance was 54·15 pF.

experiment shown in Fig. 6, 100 μM GTPγS was introduced intracellularly to a PTX-pretreated myocyte through a recording pipette, which resulted in activation of the K_{ACh} channel with a delay of about 2 min (cf. Fig. 4*A*). The time required to reach peak activation of K_{ACh} current by GTPγS after establishing the whole-cell configuration (break-in) was 6·6 ± 0·9 min in the PTX-pretreated cells ($n = 6$), which is significantly longer than the time (2·5 ± 0·1 min, $n = 13$) required in control (PTX untreated) cells (cf. Fig. 4). It has been suggested that PTX-mediated ADP-ribosylation of $G_K\alpha$ stabilizes its binding to GDP and slows the exchange of GDP bound to $G_K\alpha$ for GTPγS (Yatani, Okabe, Polakis, Halenbeck, McCormick & Brown, 1990). This characteristic of the modified $G_K\alpha$ subunit appears to underlie the slower onset of GTPγS-induced K_{ACh} current activation in PTX-pretreated cells (Fig. 6*A*).

Bath application of 10 μM ATP produced only an inward shift of the holding current at −40 mV, failing to evoke the transient outward shift that was observed in PTX-untreated cells in the presence of ACh (Fig. 2) or intracellular GTPγS (Fig. 4). The latter finding supports our hypothesis that the

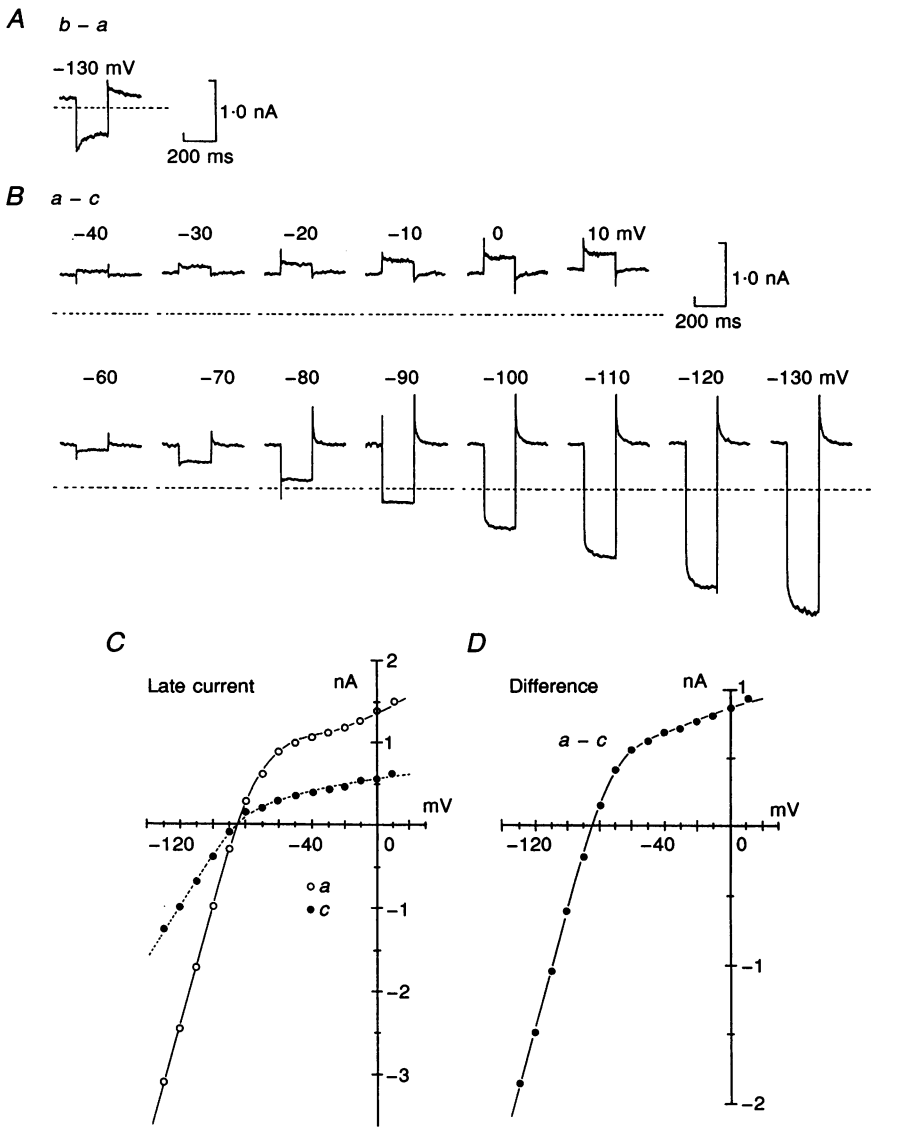

Figure 5. Inhibition of GTPγS-induced K_{ACh} current by ATP from the experiment of Fig. 4

A, difference current ($b - a$) in response to a voltage step to −130 mV recorded during the initial outward shift of the holding current upon ATP application. *B*, membrane currents inhibited by ATP ($a - c$), obtained by digital subtraction of the current trace recorded during exposure to ATP (c) from that before exposure to ATP (a), at each test potential shown above the current trace. *C*, *I–V* relationships of the late current from the records in Fig. 4*B*, before (a, ○) and during exposure to ATP (c, ●); late current levels were measured near the end of each pulse. Continuous and dashed lines through data points were fitted by eye for the current levels before (a, ○) and during exposure to ATP (c, ●), respectively. *D*, *I–V* relationship of the membrane currents inhibited by ATP ($a - c$), obtained from *B*.

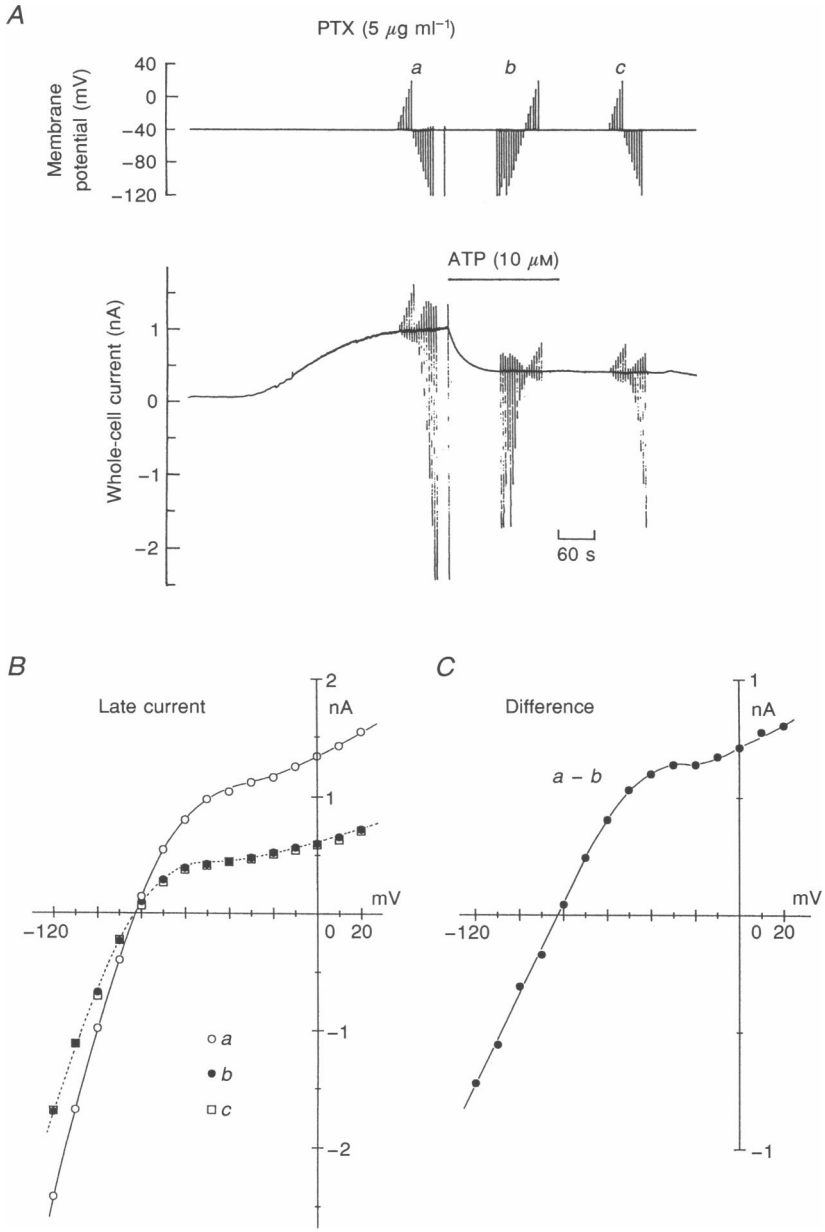

Figure 6. Involvement of a PTX-insensitive G protein in the ATP-induced inhibition of K_{ACh} current

The cell that was previously incubated at 32 °C for 2 h in a KB solution containing 5 μg ml^{-1} PTX was loaded with 100 μM GTPγS through a pipette. *A*, chart records of membrane potential (upper trace) and whole-cell current (lower trace). The chart recording of whole-cell current was begun just after the membrane patch was ruptured. The bar over the current record marks the period of external application of 10 μM ATP. Vertical lines in upper trace show imposition of 200 ms voltage pulses to potentials between +20 and −120 mV in 10 mV steps from a holding potential of −40 mV, and deflections in the lower trace represent the resulting current changes. Note that the rate of increase in outward current in association with activation of K_{ACh} current was slowed in a PTX-treated cell (cf. Fig. 4*A*). *B*, *I–V* relationships of the late current measured near the end of each clamp pulse, obtained from the data in *A*, before (*a*, ○) and during exposure to ATP (*b*, ●), and after washing out the ATP (*c*, □). Continuous and dashed lines through data points were fitted by eye for the currents recorded before (*a*, ○) and during (*b*, ●) exposure to ATP, respectively. Note that the membrane current recorded after washing out the ATP (*c*, □) was practically identical to that recorded in the presence of ATP (*b*, ●). *C*, *I–V* relationship of membrane current components inhibited by ATP, obtained by subtraction of the corresponding current records (*a* − *b*). Continuous line through data points was fitted by eye. Cell capacitance was 64·47 pF.

initial outward shift evoked by ATP either in the presence of ACh (Fig. 2) or intracellular GTPγS (Fig. 4) was due to an additional activation of K_{ACh} current, since the activating effect of ATP on K_{ACh} current is mediated by a PTX-sensitive G protein (Matsuura *et al.* 1996). Figure 6*B* illustrates the current–voltage (*I–V*) relationship of the late current recorded before (*a*, ○) and during (*b*, ●) exposure to ATP, and after withdrawal of ATP (*c*, □). The membrane current inhibited by ATP, obtained by subtraction, inwardly rectified, reversed at −83 mV (Fig. 6*C*; *a* − *b*, ●) and relaxed on voltage jumps (data not shown), demonstrating that ATP inhibited GTPγS-induced K_{ACh} current in a PTX-pretreated cell. The *I–V* relationship recorded 3 min after withdrawal of the ATP (Fig. 6*B*; *c*, □) is practically superimposable on that in the presence of ATP (Fig. 6*B*; *b*, ●), indicating that ATP produced persistent inhibition (see also Fig. 4). The degree of inhibition by ATP was 63% (0·61 nA/0·97 nA) at −40 mV in this example. In a total of four myocytes pretreated with 5 μg ml^{-1} PTX, 10 μM ATP consistently inhibited the GTPγS-induced K_{ACh} current to an extent similar to control (PTX unpretreated) cells (PTX, 66·5 ± 3·5% inhibition; control, 71·7 ± 6·3% inhibition). These results indicate that a PTX-insensitive G protein was involved in the inhibition of K_{ACh} current by external ATP.

P_2-purinoceptor subtype involved

We examined the inhibitory effects of various ATP analogues in order to identify the P_2-purinoceptor subtype involved. Figure 7 illustrates the effects of 100 μM 2-methylthio-ATP on ACh-induced K_{ACh} current. 2-Methylthio-ATP initially increased and then depressed the holding current in the presence of ACh. Figure 7*B* demonstrates the *I–V* relationships of the late current recorded before (*a*, ○) and during (*b*, ●) exposure to ACh, and after addition of 2-methylthio-ATP (*c*, □). The membrane current inhibited by 2-methylthio-ATP, obtained by subtraction, showed an inward rectification, a reversal potential of −84 mV (Fig. 7*C*; *b* − *c*, ■) and voltage-jump relaxations (data not shown), indicating that 2-methylthio-ATP inhibited ACh-induced K_{ACh} current. Over the entire voltage range 2-methylthio-ATP inhibited ACh-induced K_{ACh} current (Fig. 7*C*; *b* − *a*, ●) by about 90% without significant voltage dependence (e.g. 89·6% inhibition at −40 mV, 88·5% inhibition at −120 mV). The time required to reach peak inhibition after application of 100 μM 2-methylthio-ATP was 158·3 ± 19·6 s ($n = 4$),

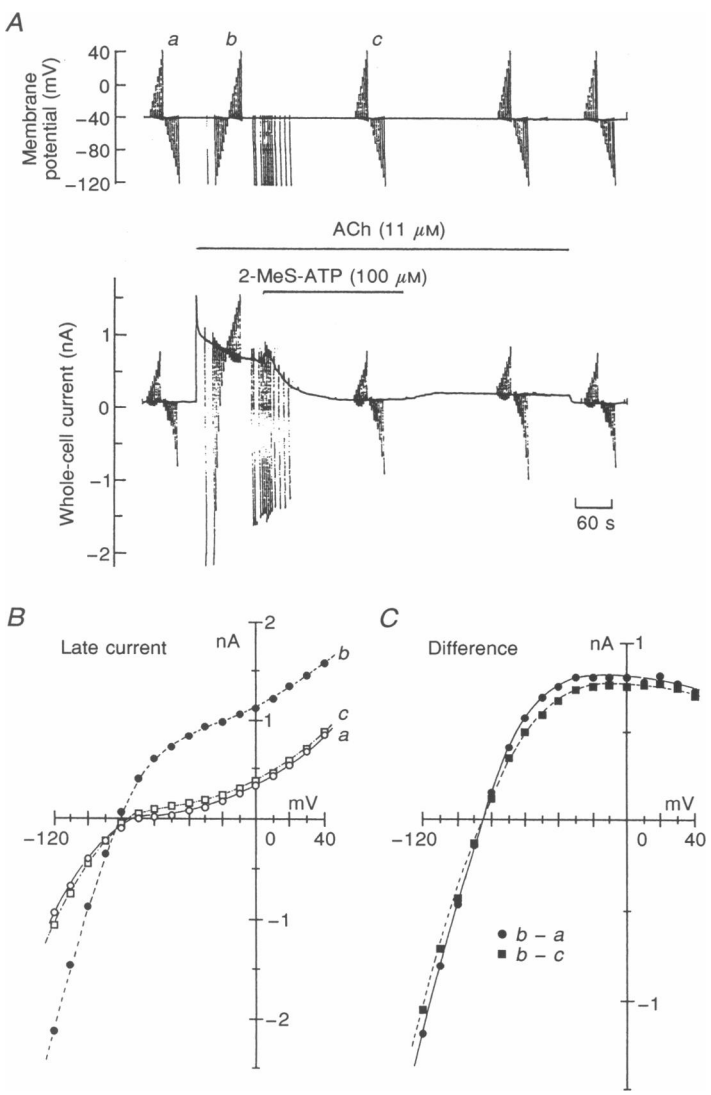

Figure 7. Inhibition of ACh-induced K_{ACh} current by 2-methylthio-ATP

A, chart record of membrane potential (upper trace) and whole-cell current (lower trace). Periods of exposure to 11 μM ACh and 100 μM 2-methylthio-ATP (2-MeS-ATP) are indicated by the horizontal bars over the current record. Vertical lines *a*, *b* and *c* indicate application of 200 ms voltage pulses to potentials between +40 and −120 mV. *B*, *I–V* relationship of late current, measured near the end of each test pulse, before (*a*, ○) and during (*b*, ●) exposure to ACh, and after addition of 2-methylthio-ATP (*c*, □). *C*, difference *I–V* relationships obtained by subtraction: ●, ACh-induced current (*b* − *a*); and ■, membrane current inhibited by 2-methylthio-ATP (*b* − *c*). Cell capacitance was 62·73 pF.

which was longer than that for 100 μM ATP (63·0 ± 2·6 s, $n = 5$, cf. Fig. 2*A*).

Figure 8*A* demonstrates the concentration–response relationship for the inhibition of ACh-induced K_{ACh} current by ATP (●), 2-methylthio-ATP (■) and α,β-methylene-ATP (▲). The data were well described by a Hill equation with the following parameters: $K_{½} = 5·5$ μM, $n_H = 0·86$, $I_{max} = 104\%$ for ATP; $K_{½} = 8·2$ μM, $n_H = 0·82$, $I_{max} = 100\%$ for 2-methylthio-ATP; $K_{½} = 8·4$ μM, $n_H = 0·81$, $I_{max} = 90\%$ for α,β-methylene-ATP; where $K_{½}$ is the concentration of ATP analogue giving half-maximal inhibition, I_{max} is the maximum degree of inhibition and n_H is the Hill coefficient. The rank potency order of ATP ⩾ 2-methylthio-ATP ⩾ α,β-methylene-ATP was consistent with the involvement of the P_{2Y}-type purinoceptor in the response. It should be noted, however, that the differences in both maximal effects and $K_{½}$ values for the inhibition of K_{ACh} current among these three agonists were small, indicating that they were nearly equipotent in producing an inhibitory effect. Figure 8*B* illustrates the dose-dependent inhibition by ATP of GTPγS-induced K_{ACh} current, which was well fitted by a Hill equation with $K_{½} = 4·5$ μM, $n_H = 1·02$ and $I_{max} = 95\%$. The concentration–response curve for the ATP block of GTPγS-induced K_{ACh} current did not differ significantly from that for the ACh-induced current (Fig. 8*A* and *B*). Maximum inhibition by ATP of the ACh-induced current (96·3 ± 8·1%, $n = 5$) was slightly greater (statistically insignificant) than that of the GTPγS-induced current (90·0 ± 5·1%, $n = 3$).

Signal transduction pathways involved in P_2-purinoceptor-induced K_{ACh} current inhibition

Is a second messenger involved? Stimulation of P_2-purinoceptors inhibited K_{ACh} current probably by activating a PTX-insensitive G protein (Figs 4, 5 and 6). To determine whether an intracellular diffusible second messenger is involved in the P_2-purinergic inhibition of K_{ACh} current, single-channel current recordings were made in the cell-attached configuration. If ATP exerts its inhibitory effects by activating some type of intracellular second messenger(s), ATP added to the bath should be effective in reducing the activity of the K_{ACh} channel in a cell-attached membrane patch isolated from the bath solution by the gigaohm seal.

Figure 9*A* illustrates a continuous recording of single K_{ACh} channel current activated by 1 μM ACh in the pipette before and during bath application of 100 μM ATP. Since the activities of the K_{ACh} channel rapidly declined during the initial 20 s following cell-attached patch formation (Kim, 1991*c*), the effects of ATP were tested after the activity reached a steady state. Bath application of ATP gradually reduced the activities of the ACh-induced K_{ACh} channel, which recovered after withdrawal of ATP (Fig. 9*A*). To quantitatively evaluate channel activity before and during bath application of ATP, the mean patch current ($I = NP_o i$), obtained by integrating the amplitude histogram (not shown), was divided by the unit amplitude of the single-channel current (i) to yield NP_o (I/i), where N is the total number of channels active within the patch and P_o is the

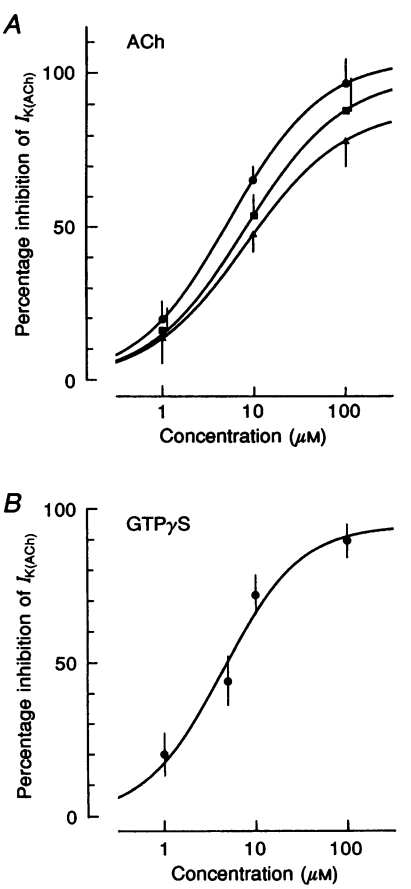

Figure 8. Concentration–response relationship for the inhibition of K_{ACh} current ($I_{K(ACh)}$) by ATP, 2-methylthio-ATP and α,β-methylene-ATP

A, the cell was initially exposed to 11 μM ACh to maximally activate K_{ACh} current and then to various concentrations of ATP analogues until a steady degree of inhibition was observed. The percentage inhibition represents the magnitude of the inward current shift at −40 mV caused by ATP (●), 2-methylthio-ATP (■) and α,β-methylene-ATP (▲) with reference to the previous outward current level produced by ACh. In order to avoid possible contamination by the time-dependent decrease of ACh-induced K_{ACh} current, data were obtained from the cell in which ACh-induced K_{ACh} current desensitized slowly, especially for the test of 1 μM. Each point is the mean of 3–6 cells and error bars indicate 1 S.E.M. The curve was drawn by a least-squares fit of the Hill equation:

$$I = I_{max}/\{1 + (K_{½}/[\text{agonist}])^{n_H}\},$$

where I_{max} is maximum degree of inhibition expressed as a percentage, $K_{½}$ is the concentration of ATP analogue causing half-maximal inhibition (IC_{50}) and n_H is the Hill coefficient. For ATP, $K_{½} = 5·5$ μM, $n_H = 0·86$ and $I_{max} = 104$. For 2-methylthio-ATP, $K_{½} = 8·2$ μM, $n_H = 0·82$ and $I_{max} = 100$. For α,β-methylene-ATP, $K_{½} = 8·4$ μM, $n_H = 0·81$ and $I_{max} = 90$. *B*, the percentage inhibition of GTPγS-induced K_{ACh} current by ATP, obtained by normalizing the magnitude of the inward current shift at −40 or −50 mV caused by ATP with reference to the amplitude of the previous outward current shift caused by GTPγS, was fitted with the same equation as that used in *A*, with $K_{½} = 4·5$ μM, $n_H = 1·02$ and $I_{max} = 95$. Data are expressed as means ± S.E.M. of 3–4 cells.

probability of the channel being open. Figure 9*B* illustrates changes in the NP_o value observed in the experiment shown in Fig. 9*A*. ATP reduced the NP_o by 61·9% (0·105 before ATP application, 0·04 during its application) in this example. The unit amplitude of the channel current, measured in the amplitude histogram, was not affected by exposure to ATP (4·42 pA before ATP application, 4·28 pA during its application). Thus, bath application of ATP reduced the activities of the K_{ACh} channel by decreasing the channel opening frequency without affecting the unitary current amplitude. This result suggests the possible involvement of a cytosolic second messenger in the inhibition of the K_{ACh} channel. It should be noted, however, that such an ATP inhibition of the channel activity was not always observed. We could detect an ATP-induced reduction of the ACh-activated K_{ACh} channel activity in two out of eight patches examined. In the remaining six patches, ATP was without effect; this could be related to the limited diffusion of a possible second messenger to the membrane patch sucked into the pipette. The inhibition of the single-channel activities by 100 μM ATP in a cell-attached patch (59·2 ± 2·8% inhibition, $n = 2$) was less pronounced than 100 μM ATP-induced inhibition of whole-cell current (96·3 ± 8·1% inhibition, $n = 5$; cf. Figs 2 and 8), which may also be associated with the limited accessibility of a possible second messenger to the membrane patch.

Are intracellular Ca^{2+} or protein kinase C involved? In rabbit heart, the P_2-purinoceptor is suggested to be coupled to the activation of phospholipase C (Takikawa, Kurachi, Mashima & Sugimoto, 1990), which may lead to the generation of two second messengers: inositol 1,4,5-trisphosphate ($InsP_3$), which mobilizes Ca^{2+}, and diacylglycerol (DAG), which activates protein kinase C. The finding that P_2-purinoceptor stimulation inhibited K_{ACh} current in cells

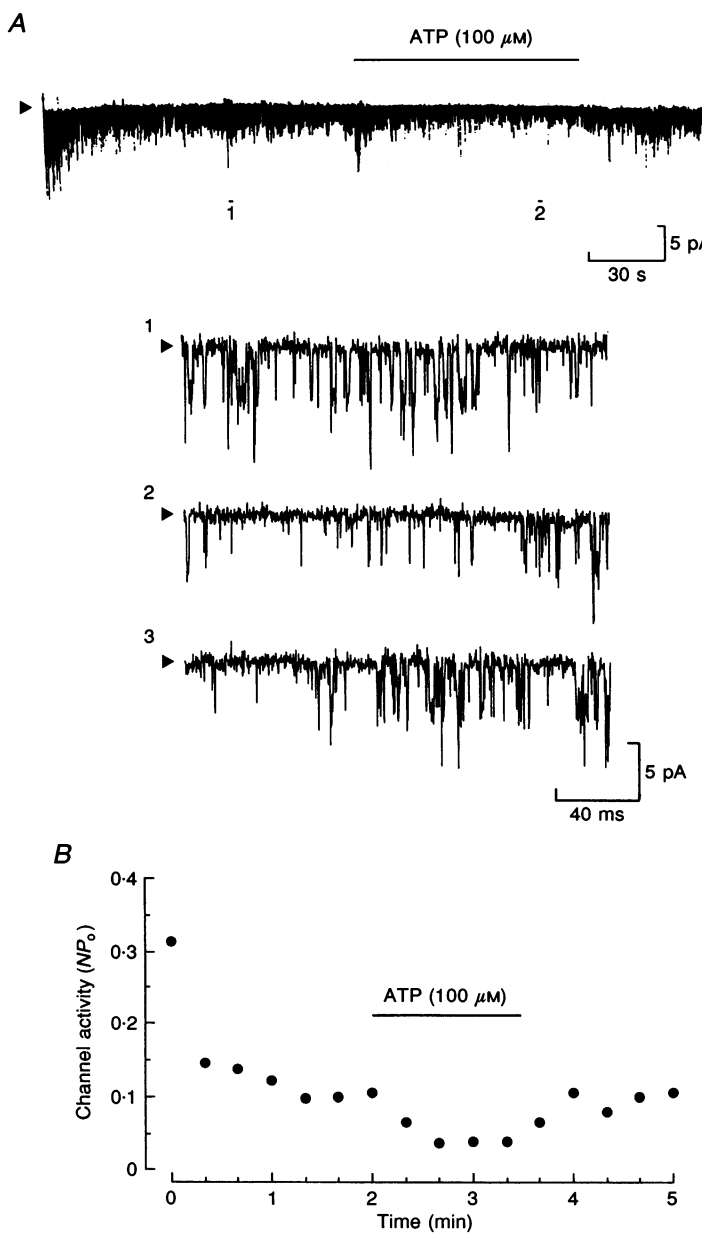

Figure 9. Inhibition of K_{ACh} channel activities by bath application of ATP

A, chart record of the K_{ACh} channel currents from a cell-attached patch activated by 1 μM ACh in the pipette at the resting membrane potential (assumed to be approximately −80 mV). ATP (100 μM) was added to the bath solution (normal Tyrode solution) during the period indicated by the horizontal bar over the chart record. Expanded current traces in the lower panel were recorded at points marked 1, 2 and 3 on the chart record. Zero current level is indicated by arrowheads to the left of each row. *B*, channel activity, represented as mean NP_o during 4·096 s periods, plotted as a function of time for the entire experiment.

internally dialysed with 5 mM EGTA (pCa = 10·2, Figs 1–7) suggests that intracellular Ca^{2+} did not play an essential role in mediating the inhibitory effects. In addition, a similar extent of inhibition was observed in cells loaded with 20 mM BAPTA (Tsien, 1980), a much faster and stronger Ca^{2+} chelator. In the presence of 20 mM BAPTA (pCa = 10·7), 100 μM ATP inhibited K_{ACh} current induced by ACh (11 μM) at −40 mV by 94·8 ± 5·7% ($n = 3$), a value similar to that observed with control 5 mM EGTA (96·3 ± 8·1%, $n = 5$), showing that the inhibitory effect of ATP was not affected by an increased Ca^{2+} buffering capacity. These results indicate that external ATP inhibited K_{ACh} current through a mechanism independent of intracellular Ca^{2+}.

To test whether protein kinase C was involved, we examined the inhibitory effects of P_2-purinoceptor stimulation on K_{ACh} current in cells loaded intracellularly with 20 μM H-7, a protein kinase C inhibitor. A blockade of protein kinase C activities after this H-7 loading was confirmed by the inability of 12-*O*-tetradecanoylphorbol-13-acetate (TPA, 0·1 μM), an activator of protein kinase C, to enhance the delayed rectifier K^+ current (data not shown). In the presence of 20 μM H-7, 100 μM ATP still inhibited K_{ACh} current induced by ACh (11 μM) by about 90% over the entire voltage range. In a total of three myocytes loaded with 20 μM H-7, 100 μM ATP inhibited ACh-induced K_{ACh} current at −40 mV by 89·7 ± 3·5%. This value does not differ significantly from the value observed in control cells (96·3 ± 8·1%, $n = 5$), suggesting that activation of protein kinase C was not primarily involved in the P_2-purinoceptor-induced K_{ACh} current inhibition.

DISCUSSION

The major findings of the present investigation are: (a) in addition to its membrane-delimited activation via G_K (Matsuura *et al.* 1996), extracellular ATP triggers a second inhibitory reaction on the cardiac K_{ACh} channels through a P_{2Y}-type purinoceptor; (b) P_{2Y}-purinergic inhibition of the K_{ACh} channel appears to involve a PTX-insensitive G protein and a cytosolic second messenger which interferes with the signal from activated G_K subunits to the K_{ACh} channel protein.

Activation of K_{ACh} current by a high concentration of ATP is characterized by its monotonic decrease to a steady level below the pre-drug level in 1–2 min in guinea-pig atrial myocytes (Fig. 1). Based on the previous (Matsuura *et al.* 1996) and present investigations, it is suggested that extracellular ATP not only directly (in a 'membrane-delimited' manner) activates but also indirectly (via a second messenger) inhibits the K_{ACh} channel. In general, the agonist-mediated response through a direct G protein interaction with an ion channel takes place more rapidly than that evoked via a diffusible second messenger (Osterrider, Yang & Trautwein, 1981; Yatani & Brown, 1989). In agreement with this presumption, ATP-induced inhibition of ACh-activated K_{ACh} current, which is probably mediated by a cytoplasmic pathway, requires 63·0 ± 2·6 s to attain peak response (Fig. 2), whereas ATP-induced activation of K_{ACh} current that is via a membrane-delimited pathway reaches its peak response in 2·5 ± 0·2 s (Fig. 1). It seems reasonable, therefore, to speculate that a characteristic monotonic decrease of ATP-induced K_{ACh} current below the control level (Fig. 1) arises primarily from a gradual inhibition by ATP of the basal and ATP-activated K_{ACh} channels. Such an inhibitory mechanism of the K_{ACh} channel has not been shown to be activated following stimulation of muscarinic or P_1-purinergic receptors, in connection with the fading of ACh- or adenosine-induced K_{ACh} current. Previous studies have demonstrated that the fading of ACh-induced K_{ACh} current involves phosphorylation of the muscarinic receptor (Carmeliet & Mubagwa, 1986; Kwatra & Hosey, 1986), functional alteration of G_K (Kurachi *et al.* 1987) or dephosphorylation of the K^+ channel protein possibly by Ca^{2+}–calmodulin-dependent phosphatase (Kim, 1991*c*).

Inhibition by ATP of the basal (Fig. 1) and ACh-induced K_{ACh} current (Figs 2 and 3) was at least partly reversible with GTP in the pipette. On the other hand, a non-hydrolysable GTP analogue, GTPγS, when loaded into the cell produced an irreversible inhibition of K_{ACh} current following P_{2Y}-purinoceptor stimulation (Figs 4 and 5). These observations, in the light of the known actions of the non-hydrolysable GTP analogue (Jakobs *et al.* 1983; Gilman, 1987), strongly suggest the involvement of a G protein in the inhibition of K_{ACh} current. The PTX-pretreatment did not affect the inhibitory actions of P_{2Y}-purinoceptors on K_{ACh} current (Fig. 6), indicating that the G protein involved in this inhibition is PTX insensitive. By contrast, a PTX-sensitive G protein, G_K, was shown to couple a P_2-purinoceptor (its subtype was not identified) to the K_{ACh} channel within the atrial cell membrane (Matsuura *et al.* 1996), as an activation mechanism. It remains to be elucidated whether two antagonistic actions of ATP on the K_{ACh} channels are evoked either through distinct P_2-purinoceptors coupled to distinct G proteins or via a single P_2-purinoceptor (i.e. P_{2Y}-purinoceptor) that is coupled to divergent G proteins. This point will be clarified when truly selective antagonists for P_2-purinoceptor subtypes become available.

A P_{2Y}-purinoceptor has recently been cloned from a chick whole-brain complementary DNA library (Webb *et al.* 1993). Structural predictions suggest that the protein (362 amino acids long) possesses common features of the G protein-coupled receptor (GCR) superfamily, such as (a) seven hydrophobic transmembrane domains, (b) two consensus N-linked glycosylation sites near the N-terminus, and (c) several potential phosphorylation sites (serine and threonine residues) near the C-terminus. Depending on the cell types, the P_{2Y}-purinoceptor is shown to be coupled to either a PTX-sensitive (bovine aortic endothelial cell: Pirotton, Erneux & Boeynaems, 1987) or a PTX-insensitive G protein (rat hepatocytes: Irving & Exton, 1987; chick

myotubes: Haggblad & Heilbronn, 1988; ferret cardiac myocytes: Qu, Campbell & Strauss, 1993).

Inhibition of K_{ACh} channel activity by ATP applied outside the cell-attached patch (Fig. 9) suggests that some type of cytosolic diffusible second messenger(s) is produced upon ATP application. While the second messenger system involved is presently not clear, our experiments using either (i) 20 μM H-7 or (ii) 20 mM BAPTA suggest that protein kinase C and intracellular Ca^{2+} are not essential for mediating the inhibitory effect of ATP. The experimental results obtained by loading GTPγS into the cell (Figs 4–6) provide important information concerning the inhibition site. In the presence of GTPγS, G_K is dissociated into a GTPγS-bound α subunit, $G_K\alpha_{GTP\gamma S}$ and a $G_K\beta\gamma$ subunit and reassociation of a $G_K\alpha_{GTP\gamma S}$ with a $G_K\beta\gamma$ subunit is prevented. Under this condition a $G_K\beta\gamma$ subunit persistently activates the K_{ACh} channel (Logothetis *et al.* 1987; for review, see Kurachi, 1995). The ATP-induced inhibition of the GTPγS-activated K_{ACh} current, therefore, indicates that the interaction between an activated $G_K\beta\gamma$ subunit and the K_{ACh} channel protein is disrupted following P_{2Y}-purinoceptor activation. While it remains unknown how the signal from a $G_K\beta\gamma$ subunit to the channel is blocked, a functional alteration of a $G_K\beta\gamma$ subunit or the K_{ACh} channel protein, or both, may be induced. Similar disruption of the interaction between an activated PTX-sensitive G protein and the G protein-gated K^+ channel has recently been found to be evoked by phosphorylation of the K^+ channel by protein kinase C in rat brain neurons (Takano, Stanfield, Nakajima & Nakajima, 1995). Further studies are necessary to elucidate the mechanisms mediating the inhibitory effect of the P_{2Y}-purinoceptor on the K_{ACh} channel.

ATP is co-released along with principal neurotransmitters during the stimulation of both sympathetic and parasympathetic nerves and acts as an active neurotransmitter (for review see Gordon, 1986; Burnstock, 1986). In addition, ATP was shown to be released from various cell types, such as aggregating platelets, vascular endothelial cells and cardiac cells (Clemens & Forrester, 1980), under certain conditions (for review see Gordon, 1986). It is therefore probable that under both physiological and pathophysiological conditions ATP released extracellularly may produce a dual effect on sino-atrial node activity, atrioventricular node conduction and atrial contractility by affecting the K_{ACh} channel activities. External application of ATP slows the atrioventricular conduction in guinea-pig or human heart, although this effect is thought to involve activation of P_1-purinoceptors by adenosine, which is formed upon ATP hydrolysis by ecto-5′-nucleotidase (Belardinelli, Shryock, West, Clemo, DiMarco & Berne, 1984). On the other hand, in the presence of theophylline, a P_1-purinoceptor inhibitor, extracellular ATP was demonstrated to accelerate the sinus pacemaker rhythm and atrioventricular conduction in the rabbit heart under Langendorff perfusion (Takikawa *et al.* 1990). In addition, these effects were not affected by PTX pretreatment but were blocked by apamin, a P_2-purinoceptor antagonist, thus showing that external ATP produces a stimulatory effect on sino-atrial node activity and atrioventricular conduction via a PTX-insensitive pathway by binding to an ATP-specific P_2-purinoceptor. These results are consistent with the present observation that ATP inhibits K_{ACh} channels via a PTX-insensitive mechanism. It will be interesting to examine the effects of extracellular ATP on membrane currents in the sino-atrial and atrioventricular node cells in relation to the positive chronotropic and dromotropic effects caused by P_2-purinoceptor stimulation.

Belardinelli, L., Shryock, J., West, G. A., Clemo, H. F., DiMarco, J. P. & Berne, R. M. (1984). Effects of adenosine and adenosine nucleotides on the atrioventricular node of isolated guinea pig hearts. *Circulation* **70**, 1083–1091.

Breitwieser, G. E. & Szabo, G. (1985). Uncoupling of cardiac muscarinic and β-adrenergic receptors from ion channels by a guanine nucleotide analogue. *Nature* **317**, 538–540.

Burnstock, G. (1986). Purines as cotransmitters in adrenergic and cholinergic neurons. *Progress in Brain Research* **68**, 193–203.

Carmeliet, E. & Mubagwa, K. (1986). Desensitization of the acetylcholine-induced increase of potassium conductance in rabbit cardiac Purkinje fibres. *Journal of Physiology* **371**, 239–255.

Clemens, M. G. & Forrester, T. (1980). Appearance of adenosine triphosphate in the coronary sinus effluent from isolated working rat heart in response to hypoxia. *Journal of Physiology* **312**, 143–158.

Fabiato, A. & Fabiato, F. (1979). Calculator programs for computing the composition of the solutions containing multiple metals and ligands used for experiments in skinned muscle cells. *Journal de Physiologie* **57**, 463–505.

Gilman, A. G. (1987). G proteins: transducers of receptor-generated signals. *Annual Review of Biochemistry* **56**, 615–649.

Gordon, J. L. (1986). Extracellular ATP: effects, sources and fate. *Biochemical Journal* **233**, 309–319.

Haggblad, J. & Heilbronn, E. (1988). P_2-purinoceptor-stimulated phosphoinositide turnover in chick myotubes. Calcium mobilization and the role of guanyl nucleotide-binding proteins. *FEBS Letters* **235**, 133–136.

Hamill, O. P., Marty, A., Neher, E., Sakmann, B. & Sigworth, F. J. (1981). Improved patch-clamp techniques for high-resolution current recording from cells and cell-free membrane patches. *Pflügers Archiv* **391**, 85–100.

Hirano, Y., Abe, S., Sawanobori, T. & Hiraoka, M. (1991). External ATP-induced changes in $[Ca^{2+}]_i$ and membrane currents in mammalian atrial myocytes. *American Journal of Physiology* **260**, C673–680.

Hwang, T.-C., Horie, M., Nairn, A. G. & Gadsby, D. C. (1992). Role of GTP-binding proteins in the regulation of mammalian cardiac chloride conductance. *Journal of General Physiology* **99**, 465–489.

Irving, H. R. & Exton, J. H. (1987). Phosphatidylcholine breakdown in rat liver plasma membranes. Roles of guanine nucleotides and P_2-purinergic agonists. *Journal of Biological Chemistry* **262**, 3440–3443.

Isenberg, G. & Klöckner, U. (1982). Calcium tolerant ventricular myocytes prepared by preincubation in a 'KB medium'. *Pflügers Archiv* **395**, 6–18.

JAKOBS, K. H., GEHRING, U., GAUGLER, B., PFEUFFER, T. & SCHULTZ, G. (1983). Occurrence of an inhibitory guanine nucleotide-binding regulatory component of the adenylate cyclase system in cyc$^-$ variants of S49 lymphoma cells. *European Journal of Biochemistry* **130**, 605–611.

KIM, D. (1991*a*). Calcitonin-gene-related peptide activates the muscarinic-gated K^+ current in atrial cells. *Pflügers Archiv* **418**, 338–345.

KIM, D. (1991*b*). Endothelin activation of an inwardly rectifying K^+ current in atrial cells. *Circulation Research* **69**, 250–255.

KIM, D. (1991*c*). Modulation of acetylcholine-activated K^+ channel function in rat atrial cells by phosphorylation. *Journal of Physiology* **437**, 133–155.

KURACHI, Y. (1995). G protein regulation of cardiac muscarinic potassium channel. *American Journal of Physiology* **269**, C821–830.

KURACHI, Y., NAKAJIMA, T. & SUGIMOTO, T. (1986). On the mechanism of activation of muscarinic K^+ channels by adenosine in isolated atrial cells: involvement of GTP-binding proteins. *Pflügers Archiv* **407**, 264–274.

KURACHI, Y., NAKAJIMA, T. & SUGIMOTO, T. (1987). Short-term desensitization of muscarinic K^+ channel current in isolated atrial myocytes and possible role of GTP-binding proteins. *Pflügers Archiv* **410**, 227–233.

KWATRA, M. M. & HOSEY, M. M. (1986). Phosphorylation of the cardiac muscarinic receptor in intact chick heart and its regulation by a muscarinic agonist. *Journal of Biological Chemistry* **261**, 12429–12432.

LEWIS, D. L. & CLAPHAM, D. E. (1989). Somatostatin activates an inwardly rectifying K^+ channel in neonatal rat atrial cells. *Pflügers Archiv* **414**, 492–494.

LOGOTHETIS, D. E., KURACHI, Y., GALPER, J., NEER, E. J. & CLAPHAM, D. E. (1987). The $\beta\gamma$ subunits of GTP-binding proteins activate the muscarinic K^+ channel in heart. *Nature* **325**, 321–326.

MATSUURA, H. & EHARA, T. (1992). Activation of chloride current by purinergic stimulation in guinea-pig heart cells. *Circulation Research* **70**, 851–855.

MATSUURA, H., SAKAGUCHI, M., TSURUHARA, Y. & EHARA, T. (1996). Activation of the muscarinic K^+ channel by P_2-purinoceptors via pertussis toxin-sensitive G proteins in guinea-pig atrial cells. *Journal of Physiology* **490**, 659–671.

OSTERRIDER, W., YANG, Q. F. & TRAUTWEIN, W. (1981). The time course of the muscarinic response to ionophoretic acetylcholine application to the S-A node of the rabbit heart. *Pflügers Archiv* **389**, 283–291.

PFAFFINGER, P. J., MARTIN, J. M., HUNTER, D. D., NATHANSON, N. M. & HILLE, B. (1985). GTP-binding proteins couple cardiac muscarinic receptors to a K channel. *Nature* **317**, 536–538.

PIROTTON, S., ERNEUX, C. & BOEYNAEMS, J. M. (1987). Dual role of GTP-binding proteins in the control of endothelial prostacyclin. *Biochemical and Biophysical Research Communications* **147**, 1113–1120.

POWELL, T., TERRAR, D. A. & TWIST, V. W. (1980). Electrical properties of individual cells isolated from adult rat ventricular myocardium. *Journal of Physiology* **302**, 131–153.

QU, Y., CAMPBELL, D. L. & STRAUSS, H. C. (1993). Modulation of L-type Ca^{2+} current by extracellular ATP in ferret isolated right ventricular myocytes. *Journal of Physiology* **471**, 295–317.

SAKMANN, B., NOMA, A. & TRAUTWEIN, W. (1983). Acetylcholine activation of single muscarinic K^+ channels in isolated pacemaker cells of the mammalian heart. *Nature* **303**, 250–253.

TAKANO, K., STANFIELD, P. R., NAKAJIMA, S. & NAKAJIMA, Y. (1995). Protein kinase C-mediated inhibition of an inward rectifier potassium channel by substance P in nucleus basalis neurons. *Neuron* **14**, 999–1008.

TAKIKAWA, R., KURACHI, Y., MASHIMA, S. & SUGIMOTO, T. (1990). Adenosine-5′-triphosphate-induced sinus tachycardia mediated by prostaglandin synthesis via phospholipase C in the rabbit heart. *Pflügers Archiv* **417**, 13–20.

TSIEN, R. Y. (1980). New calcium indicators and buffers with high selectivity against magnesium and protons: design, synthesis, and properties of prototype structures. *Biochemistry* **19**, 2396–2404.

TSIEN, R. Y. & RINK, T. J. (1980). Neutral carrier ion-selective microelectrodes for measurement of intracellular free calcium. *Biochimica et Biophysica Acta* **599**, 623–638.

WEBB, T. E., SIMON, J., KRISHEK, B. J., BATESON, A. N., SMART, T. G., KING, B. F., BURNSTOCK, G. & BARNARD, E. A. (1993). Cloning and functional expression of a brain G-protein-coupled ATP receptor. *FEBS Letters* **324**, 219–225.

YATANI, A. & BROWN, A. M. (1989). Rapid β-adrenergic modulation of cardiac calcium channel currents by a fast G protein pathway. *Science* **245**, 71–74.

YATANI, A., OKABE, K., POLAKIS, P., HALENBECK, R., MCCORMICK, F. & BROWN, A. M. (1990). *ras* p21 and GAP inhibit coupling of muscarinic receptors to atrial K^+ channels. *Cell* **61**, 769–776.

ZANG, W.-J., YU, X.-J., HONJO, H., KIRBY, M. S. & BOYETT, M. R. (1993). On the role of G protein activation and phosphorylation in desensitization to acetylcholine in guinea-pig atrial cells. *Journal of Physiology* **464**, 649–679.

Acknowledgements

We wish to thank Dr T. Shioya for providing the computer programmes used for the data analysis, and Dr L. Filippi for critically reading the manuscript. This work was supported by grants from the Ministry of Education, Science and Culture of Japan (Nos 05670048, 06670061 and 07670056) and the Naito Foundation (No. 93-147). The secretarial assistance of Ms M. Fuchigami is also appreciated.

Author's email address

H. Matsuura: matsuura@smsnet.saga-med.ac.jp

Received 22 April 1996; accepted 20 August 1996.